Horizontal Rhombic Antennas *

By E. BRUCE, A. C. BECK and L. R. LOWRY

The paper discusses the theoretical methods employed by the authors in dimensioning horizontal rhombic receiving antennas. Experimental proof is given of the engineering accuracy of the directivity calculations on which this work is based. There are included brief descriptions of the antenna-to-transmission line coupling circuits and the resistance terminations for rhombic antennas.

Introduction

AN introductory discussion has been given in a previous paper [1] of a type of antenna which maintains a desirable degree of directivity throughout a broad continuous range of frequencies. This structure was descriptively termed the "diamond-shaped" antenna in that paper, but has since become known as the "rhombic antenna" and will be so designated here.

This paper discusses, in some detail, the theoretical methods employed by the authors in dimensioning horizontal rhombic receiving antennas from data obtained by preliminary surveys of the incident-plane angles of wave-arrival at the proposed receiving site.

Experimental proof is given of the engineering accuracy of the directivity calculations on which this work is based. Checking measurements were made on small-scale rhombic antennas operating at correspondingly short wave-lengths. Confirming data were also obtained on large, adjustable rhombic antennas during the reception of European signals.

The paper also includes a brief discussion of the antenna-to-transmission line coupling circuits employed and, in addition, the resistance terminations, located at the end of the antenna remote from the receiver, used for suppressing standing waves and promoting unidirectivity. Some of the performance curves obtained on these devices are reproduced.

Antenna Dimensions

Before designing any highly directive receiving antenna system, it is desirable to have a knowledge of the direction of arrival, the angular spread, and the angular variation in direction of the waves to be

* Published in *Proc. I. R. E.*, January, 1935.

[1] "Developments in Short-Wave Directive Antennas," by E. Bruce, *Proc. I. R. E.*, August, 1931; *Bell Sys. Tech. Jour.*, October, 1931.

received. Such information has been obtained by employing the methods described by Friis, Feldman and Sharpless.[2]

In general, the principal axis of the antenna departs very little from the true bearing of the station to be received. However, the average vertical direction of the waves in the incident plane and their angular variation have an effect upon the determination of the correct dimensions of a horizontal rhombic receiving antenna.

Without careful consideration, one might be led to believe that the theoretical effectiveness of a horizontal rhombic receiving antenna would increase without limit, for a stable wave-direction, as the properly related dimensions are increased. It will be shown that, for a given incident wave-angle above the horizontal, the optimum dimensions have quite definite values.

The essential dimensions of this type of antenna are its height above ground, the length of a side element, and the inclination angle of these elements in respect to the wave-direction. At frequencies higher than about fifteen megacycles, this type of antenna is relatively so inexpensive that it is usually economically possible to select a combination of these dimensions which will produce the maximum signal output.

At lower frequencies, the increasing cost, particularly of the pole height required for maximum output, demands that a careful analysis be made of effective compromise designs. One such design method involves a sacrifice in antenna height, which sacrifice can be partially compensated for by an increase in element length. Thus the economic balance involves a weighing of supporting structure costs against the cost of land. Again, cases may arise where the recommended antenna height is practical but a sacrifice in element length is essential. The effect of this sacrifice on the directive pattern can be partially compensated for by a readjustment of the tilt-angle of the elements. The directive pattern may also be aligned with the wave-angle when both height and element length are reduced, but only at an output sacrifice.

The designer's first problem is to choose between the maximum output arrangement and the various compromise designs. In the case of a transmitting antenna, the problem is to create as large a field as possible at the distant receiving point, for a given amount of transmitter power. As long as the increase in antenna cost is smaller than the corresponding cost of an increase in transmitter power, no compromise should be made in the antenna dimensions. It is, therefore, obvious that the choice, between optimum and compromise dimensions for a transmitting antenna, is a function of the cost of the transmitter to be employed.

[2] "The Determination of the Direction of Arrival of Short Radio Waves," by H. T. Friis, C. B. Feldman and W. M. Sharpless, *Proc. I. R. E.*, January, 1934.

For a receiving antenna, the dividing line between the optimum and the compromise design methods is often defined by the relative importance, as circuit limiting factors, of static as compared with set-noise. The optimum design results in a large signal output, from the antenna, which enables the over-riding of set-noise and it also results in effective directional discrimination against static. The compromise height arrangement maintains and sometimes improves upon the directional discrimination against static but sacrifices a part of the possible antenna output-signal level. If the frequency is sufficiently low so that static rather than set-noise is practically always the circuit limitation, no real harm will result from using the compromise height design with its accompanying economic saving.

In general, compromise in element length results in a loss in both the antenna output-signal level and in static discrimination. This procedure is recommended only for exceptional cases where a restriction in available land exists, or where a broad directional characteristic is required because of a highly variable wave-direction.

Directivity Equations

In the appendix of this paper will be found the derivation, for the stated assumptions, of the three dimensional directivity equation for a horizontal rhombic receiving antenna terminated by its characteristic impedance. The principal antenna dimensions will be apparent by reference to Fig. 1.

If the horizontal component β, of the angle made by the wave-direction with the principal antenna axis, is set equal to zero in the final resulting equation in the appendix, the directivity equation for the incident plane passing through the principal axis is as follows:

$$I_R = k\left[1 + ae^{-j\left(\frac{4\pi}{\lambda}H\sin\Delta + \alpha\right)}\right] \cdot \left[\frac{\cos\phi}{1 - \sin\phi\cdot\cos\Delta}\right] \cdot \left[1 - e^{-j\frac{2\pi l}{\lambda}(1 - \sin\phi\cdot\cos\Delta)}\right]^2, \quad (1)$$

where I_R = receiver current,
k = proportionality factor,
H = height above ground,
l = wire element length,
ϕ = one-half of side apex angle,
Δ = angle made with ground by wave-direction in incident plane,
a = amplitude ratio of ground reflected field to incident field,
α = apparent phase angle lag caused by ground reflection,
λ = wave-length.

Since the principal axis of the antenna is nearly always directed toward the distant transmitter, the conditions which will maximize the above expression are of prime interest. The determination of these conditions is greatly simplified by the assumption of a perfect ground.

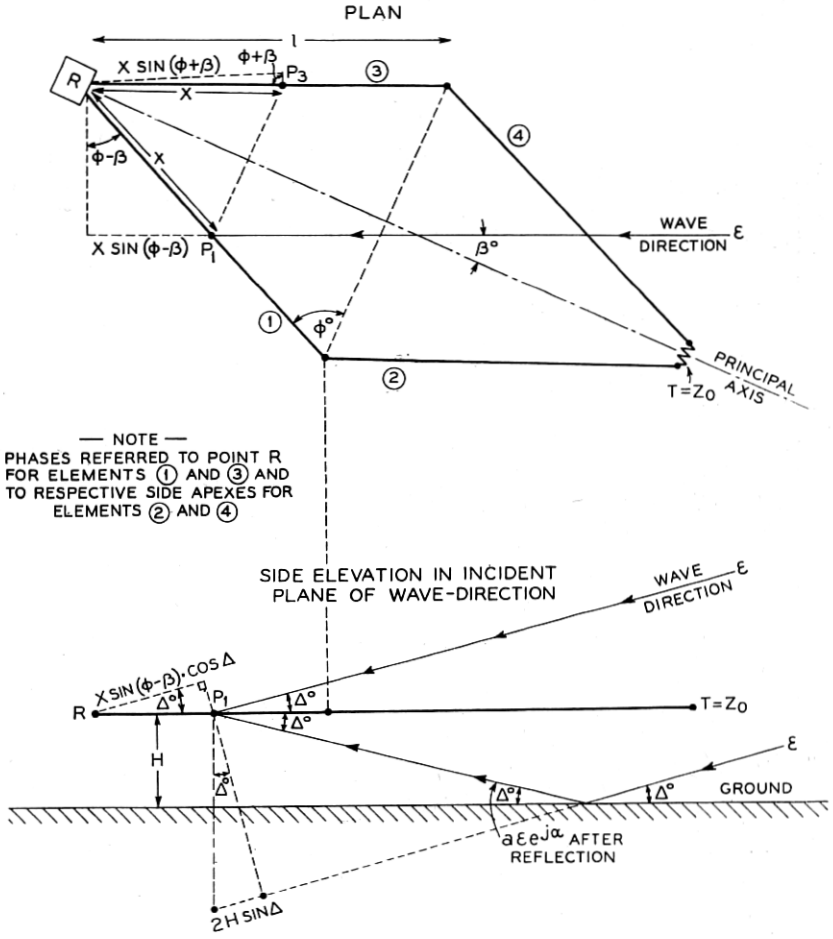

Fig. 1—Horizontal rhombic antenna dimensions.

Fortunately this is not a radical assumption for the case of horizontally polarized waves at the usual incident angles. This may be verified by reference to Fig. 2 where the values of a and α are plotted for several ordinarily encountered ground constants.

Using the perfect ground assumption, the amplitude of equation (1) is given by

$$I_R = k' \left[\sin \left(\frac{2\pi H}{\lambda} \sin \Delta \right) \right] \cdot \left[\frac{\cos \phi}{1 - \sin \phi \cdot \cos \Delta} \right] \cdot \left\{ \sin^2 \left[\frac{\pi l}{\lambda} (1 - \sin \phi \cdot \cos \Delta) \right] \right\}. \quad (2)$$

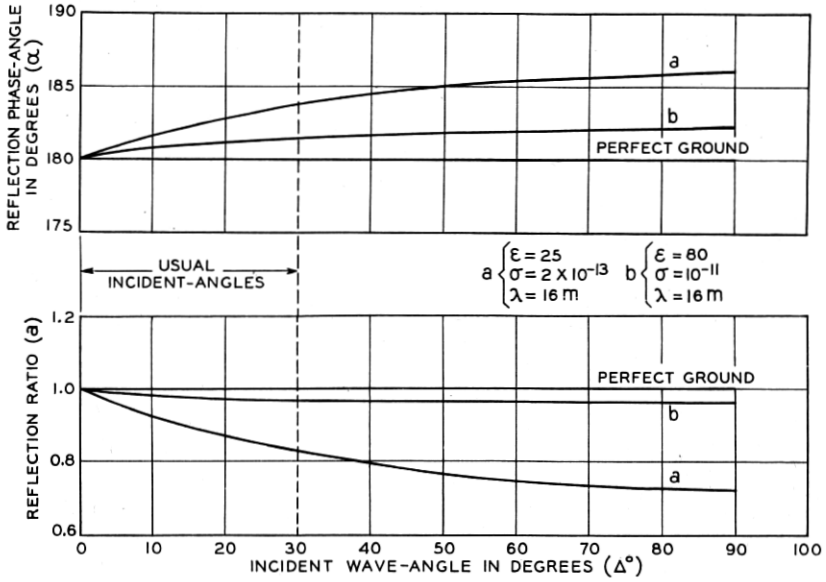

Fig. 2—Characteristics of wave-reflections from ground.

In this equation the first bracketed term may be referred to as the "height" factor, the second as the "asymmetrical directivity" factor, and the third as the "phasing" factor.

Maximum Output Design Method

In maximizing equation (2), it is necessary to deal with three variables, the antenna dimensions H, l and ϕ. Differentiating with respect to each of these variables, while holding the other two constant, and equating to zero, the following three expressions are obtained:

$\frac{\delta I_R}{\delta H} = 0$ when

$H = \frac{\lambda}{4 \sin \Delta}$ for the lowest practical height,

$\frac{\delta I_R}{\delta l} = 0$ when

$$l = \frac{\lambda}{2(1 - \sin\phi \cdot \cos\Delta)} \quad \text{for the major ear of the directive diagram,} \tag{4}$$

$\frac{\delta I_R}{\delta \phi} = 0$ when

$$\tan\left[\frac{\pi l}{\lambda}(1 - \sin\phi \cdot \cos\Delta)\right] = -\frac{2\pi l \cdot \cos^2\phi \cdot \cos\Delta(1 - \sin\phi \cdot \cos\Delta)}{\lambda(\sin\phi - \cos\Delta)}. \tag{5}$$

Substituting equation (4) into (5), it is found that,

$$\sin\phi = \cos\Delta. \tag{6}$$

This result determines the fact that, regardless of antenna height, the best tilt-angle ϕ is the complement of the wave-angle Δ, where the optimum element length is used. Taking this result and substituting it back into either (4) or (5) results in

$$l = \frac{\lambda}{2\sin^2\Delta}. \tag{7}$$

The value of "l" in equation (7) together with the height given by equation (3), and the tilt-angle given by equation (6) determine the dimensions of the horizontal rhombic antenna with maximum output for any given wave-angle Δ.

As an example of the use of the above equations, Fig. 3 is the resulting incident plane directive pattern with the antenna designed for the given wave-angle of 17.5 degrees. Figure 4 is a plot of the antenna output versus the azimuth angle for the fixed incident angle of 17.5 degrees as obtained by using these dimensions in the three-dimensional directivity equation in the appendix.

Note in Fig. 3 that the directive pattern does not have its maximum radius at the line indicating the given wave-direction even though the greatest possible amplitude for that wave-angle has been determined.

It is believed that this method of design has a definite application where over-riding set-noise by the largest possible signal output is paramount. In cases where discrimination against random static is desirable, or where the received wave-direction is unstable, an alignment of the mean wave-direction with the optimum radius of the

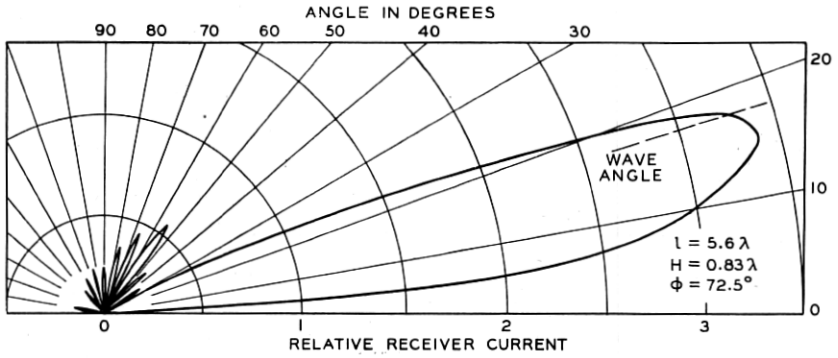

Fig. 3—Maximum output design. Receiver current diagram of incident plane directivity for a 17.5° wave-angle.

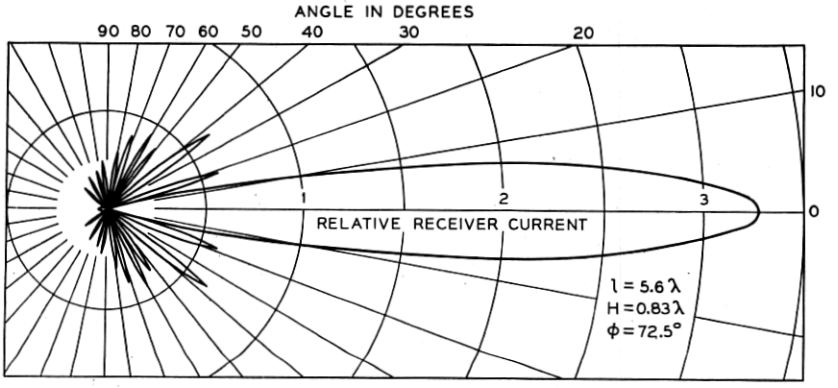

Fig. 4—Maximum output design. Receiver current versus azimuth angle for a 17.5° wave-angle.

directive diagram becomes necessary. Such an alignment can be achieved by the method described below, but only by a small sacrifice in the amplitude [3] of I_R at the required wave-angle.

The Alignment Design Method

Since by our previous method of design the height factor of equation (2) was aligned with the wave-angle, it is necessary to change either or both of the dimensions l and ϕ to secure the best output under the limiting alignment condition. This limiting condition is obtained as

[3] To compare the energy gain of one antenna with another, the amplitudes of I_R, which are proportional to effective voltages, should be corrected for the differences in radiation resistance of the antennas.

follows:

$$\frac{\delta I_R}{\delta \Delta} = 0 \text{ when}$$

$$H = \sin\phi \cdot \tan\Delta \cdot \tan\left(\frac{2\pi H}{\lambda}\sin\Delta\right) \cdot \left\{\frac{\lambda}{2\pi(1 - \sin\phi\cdot\cos\Delta)} - \frac{l}{\tan\left[\frac{\pi l}{\lambda}(1 - \sin\phi\cdot\cos\Delta)\right]}\right\}. \quad (8)$$

Substituting (3) into (8) gives

$$\tan\left[\frac{\pi l}{\lambda}(1 - \sin\phi\cdot\cos\Delta)\right] = 2\left[\frac{\pi l}{\lambda}(1 - \sin\phi\cdot\cos\Delta)\right]. \quad (9)$$

This is a transcendental equation of the form $\tan x = 2x$, whose roots, to four significant figures, are

$$x = 0, \quad 0.3710\pi, \quad 1.466\pi, \quad 2.480\pi, \quad 3.486\pi, \quad \text{etc.}$$

Alignment of the major ear of the directive pattern with the wave-angle occurs only for the first solution greater than zero. Therefore we have for this condition,

$$l = \frac{0.371\lambda}{1 - \sin\phi\cdot\cos\Delta}. \quad (10)$$

To obtain the dimensions for greatest output in the alignment design case, l and ϕ in equation (2) are no longer independent variables, but are related by equation (10). We can, therefore, eliminate either one we choose from equation (2) and maximize this new equation for the required dimensions.

Substituting (10) into (2) gives:

$$I_R' = k''\left[\sin\left(\frac{2\pi H}{\lambda}\sin\Delta\right)\right]\left[\frac{\cos\phi}{1 - \sin\phi\cos\Delta}\right] \quad (11)$$

and

$$\frac{\delta I_R'}{\delta\phi} = 0 \text{ when} \quad (12)$$

$$\sin\phi = \cos\Delta.$$

Since equation (12) is identical with equation (6), the recommended design for directive pattern alignment with the wave-angle is obtained by changing only the antenna length which was given for the maximum

output design by equation (7). By substituting (12) into (10), this becomes

$$l = \frac{0.371\lambda}{\sin^2 \Delta} . \tag{13}$$

Therefore, alignment design is obtained by the use of equations (3), (6) and (13). This shows that to change from maximum output design to alignment design it is only necessary to reduce the length to approximately seventy-four per cent of the value recommended for maximum output.

Figures 5 and 6 are examples of the directive patterns secured by such

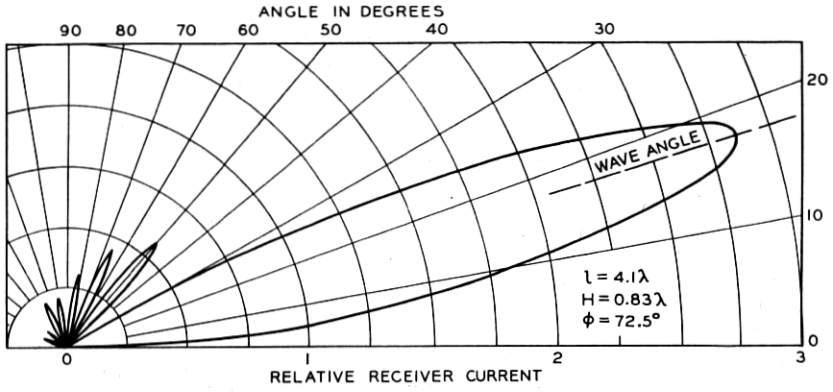

Fig. 5—Alignment design. Receiver current diagram of incident plane directivity for a 17.5° wave-angle.

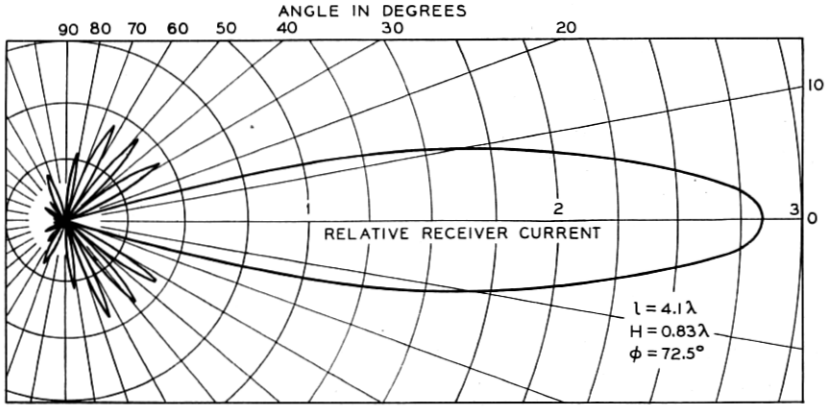

Fig. 6—Alignment design. Receiver current versus azimuth angle for a 17.5° wave-angle.

alignment design for a wave-angle of 17.5 degrees. Comparison of these diagrams with Figs. 3 and 4 shows a small loss in I_R resulting from such design. Figures 7 and 8 are similar alignment design plots for a wave-angle of 11 degrees.

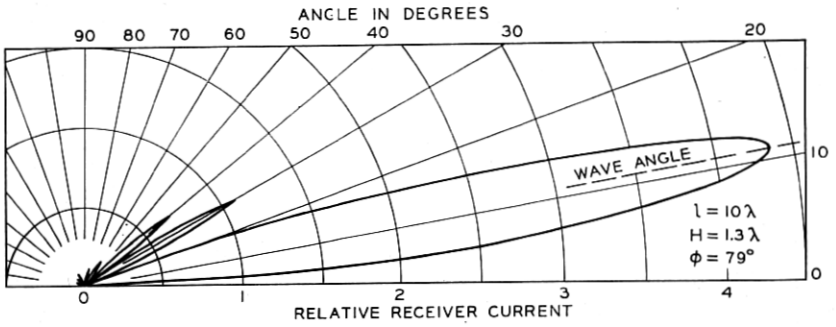

Fig. 7—Alignment design. Receiver current diagram of incident plane directivity for an 11° wave-angle.

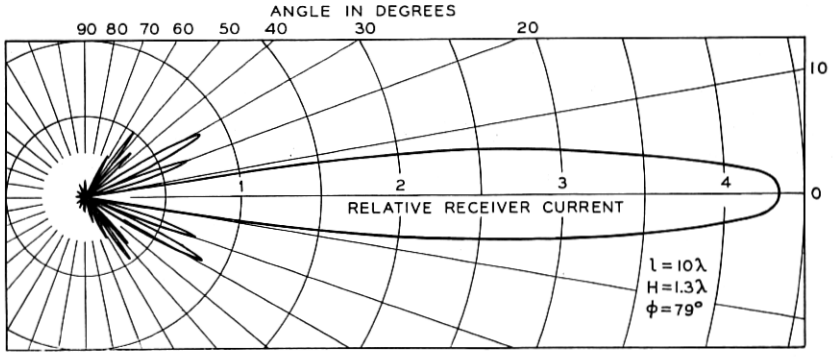

Fig. 8—Alignment design. Receiver current versus azimuth angle for an 11° wave-angle.

Compromise Design Methods

When an antenna output sacrifice must be tolerated to obtain smaller dimensions, it is often desirable to design the system for directive pattern alignment with the wave-angle, as mentioned above. The methods of accomplishing this result will now be given.

The effect on the directive pattern of reducing the height can be largely compensated for by increasing the length.

Substituting (6) into (8) gives

$$\frac{H}{\tan\left(\frac{2\pi H}{\lambda}\sin\Delta\right)} = \frac{\lambda}{2\pi\sin\Delta} - \frac{l\cdot\sin\Delta}{\tan\left(\frac{\pi l}{\lambda}\sin^2\Delta\right)}. \qquad (14)$$

When both Δ and H are specified, this equation gives the element length l to be used with the reduced height. Figures 9 and 10 are

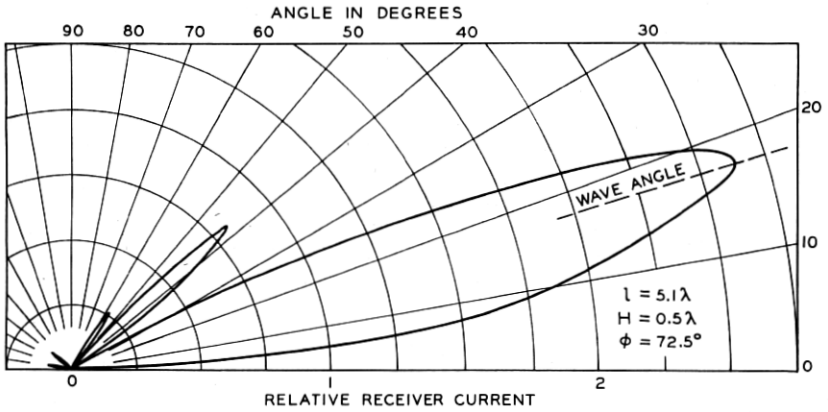

Fig. 9—Compromise height design. Receiver current diagram of incident plane directivity for a 17.5° wave-angle and a height of one-half wave-length.

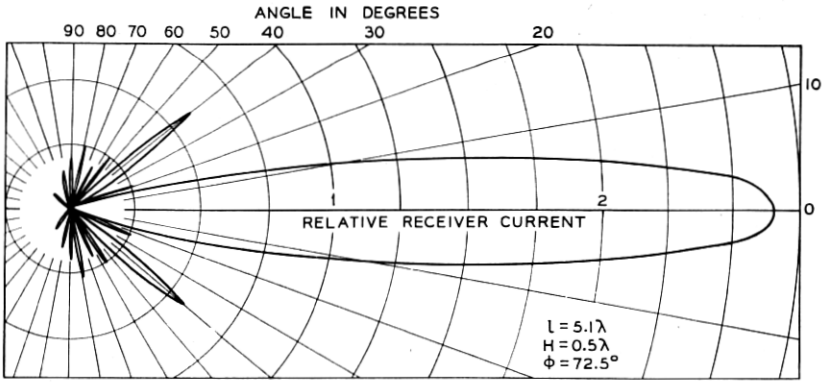

Fig. 10—Compromise height design. Receiver current versus azimuth angle for a 17.5° wave-angle and a height of one-half wave-length.

examples of the directive diagrams resulting from a reduced height of one-half wave-length and an incident wave-angle of 17.5 degrees. These last mentioned figures may be directly compared with Figs. 5

and 6 to determine what effect the sacrifice in height and the increased length has had.

The effect on the directive pattern of reducing the length can be minimized by changing the tilt-angle ϕ. When the height given by equation (3) is used, the new tilt-angle can be obtained by writing equation (10) as

$$\sin \phi = \frac{l - 0.371\lambda}{l \cos \Delta} . \tag{15}$$

If it is desired to align the directive pattern with the wave-angle when the height and length are both reduced from the recommended values, equation (8) can be solved for the new tilt-angle. Any of these compromise designs will, of course, reduce the antenna output.

Limitations of Results

The accuracy of the calculations in this paper is based on the following assumptions:

1. Negligible effect by wire attenuation.
2. Negligible mutual coupling between elements.
3. The rate of change of the effective voltage with varying dimensions is large as compared with the rate of change of radiation resistance.

The validity of the assumptions has been checked to engineering accuracies in the ultra-short wave experiments to be described, where the shape of the directivity predicted by these equations agreed well with experiment. However, theory and experiment have both shown that ordinary ground has an appreciable influence on the wire attenuation when the antenna heights are of the order of only small fractions of a wave-length. This effect increases as the antenna dimensions are extended. In such unusual cases, this behavior should be carefully investigated even though calculations including large wire attenuations have shown surprisingly little effect upon the directive diagrams. Approximate values for the variation of radiation resistance with dimensions, for terminated rhombic antennas, indicate that assumption 3 is probably warranted provided that the antenna is not extraordinarily small.

Finally, attention should be called to these important facts:

The suggested dimensions in this paper not only do not restrict the broad frequency range of this type of antenna but are in many cases

the broadest arrangements under the prescribed conditions. This statement is based on a large number of calculated directive diagrams, for various frequencies, and has been substantiated by operating tests.

Also, in certain applications, as with ultra-short waves where the direction of wave propagation is substantially horizontal ($\Delta = 0$), the derived equations place no restrictions on the antenna size.

Experimental Checks of Directivity Calculations

One method employed for experimentally checking the calculations of directivity was by means of a model small enough to permit continuous rotation of the antenna in respect to a fixed wave-direction. A simple transmitter and a double-detection receiving set, which employed a calibrated intermediate frequency attenuator, both operating at about four meters, were utilized for this work. Even at these wave-lengths, the physical dimensions of the antenna were rather large so that it was necessary to build an antenna smaller in wave-length dimensions than is usually recommended for commercial installations. As previously stated, any antenna for regular service would be designed for its own specific conditions, so that this antenna is not to be taken as a recommended design. However, this fact had no bearing on the results of these tests, for there was no intention of using this movable antenna for any purpose other than experimentally checking the directivity equations.

A photograph of the test installation is shown in Fig. 11. The antenna wires were mounted on a lattice work cross of light weight wood suspended by a system of ropes from two wooden poles. This permitted the hoisting of the entire antenna system to any height up to several wave-lengths, and rotating it to any desired angular position. The antenna is shown in more detail in the photograph of Fig. 12. It was constructed of two space-tapered wires in parallel, spaced in order to lower the antenna impedance to permit the matching of the open-wire transmission line which was attached to one end. Each element was three and a quarter wave-lengths long. The receiving set was placed in a small push-cart at the other end of the transmission line so that the line length did not need to be changed with antenna movements. An antenna of this size had a measured gain of fourteen decibels over a half-wave horizontal dipole at the same height.

The horizontal plane directive pattern was experimentally determined by measuring the antenna angle and signal output at each maximum and minimum and at fixed angles on the major lobe, as the antenna was rotated about its vertical axis. The pattern measured

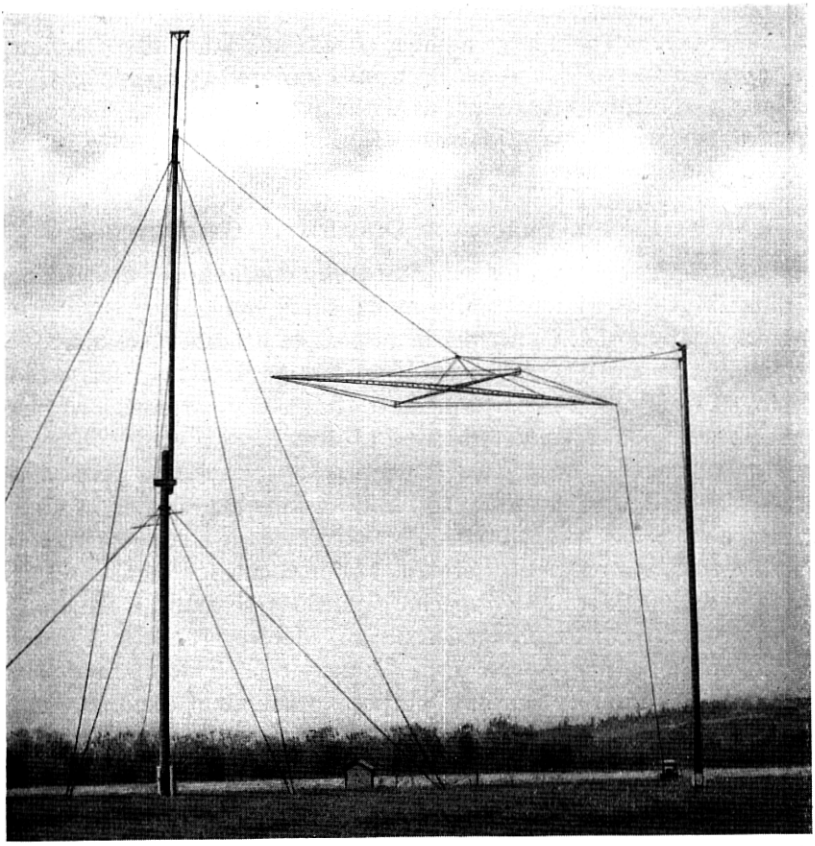

Fig. 11—Test antenna used at four meters for experimental checks of directivity calculations.

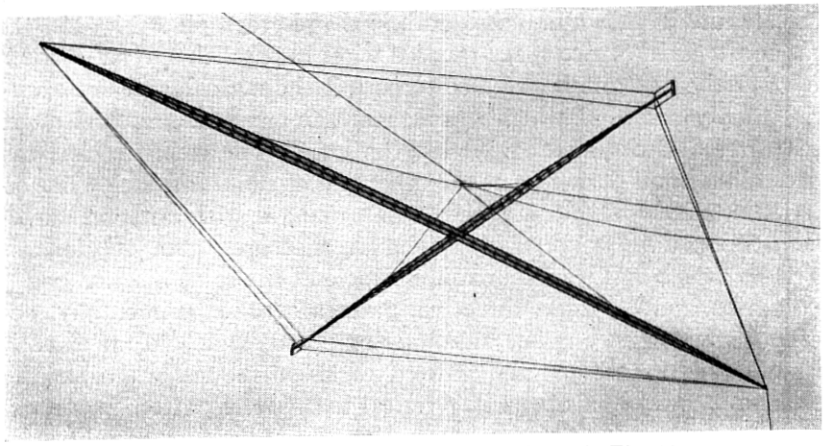

Fig. 12—A detail view of the antenna shown in Fig. 11.

in this manner is shown in Fig. 13. In this figure is also shown, for comparison purposes, the pattern calculated for these conditions by the equations derived in the appendix. The agreement between these two patterns is quite evident.

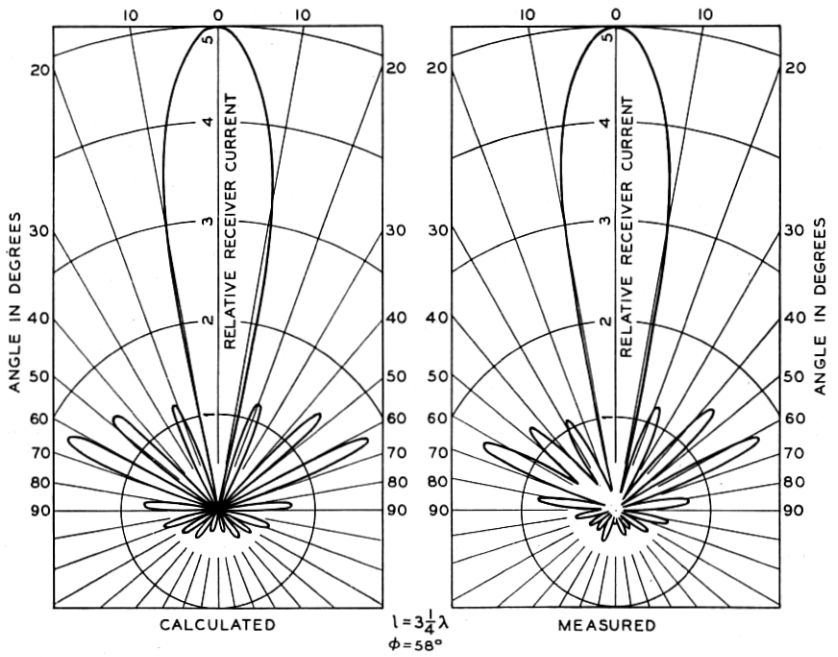

Fig. 13—Receiver current diagrams of test antenna output current versus azimuth angle for a 2.7° wave-angle.

To check the vertical directivity of the system, a portable oscillator was raised from the ground to the top of a one-hundred foot pole in front of the antenna. Due to the limited range of arrival angles so obtained, only the major lobe of the directive pattern could be traced out. Figure 14 gives the calculated major lobe for these conditions (equations corrected to actual path length difference between direct and reflected waves) with the antenna one-half wave-length above ground, and Fig. 15 is the pattern at a height of one wave-length. The circles on these curves are the measured values. These patterns show that the directivity does not change very rapidly with changes in antenna height.

Experimental checks of these directivity calculations have also been obtained on the larger antennas ordinarily used for long distance reception. A large horizontal rhombic antenna was constructed with a

motor driven winch to adjust its interior angles, thus providing control of the directivity of the antenna. This antenna could be "steered" so that either the major lobe or the first null could be used to receive or

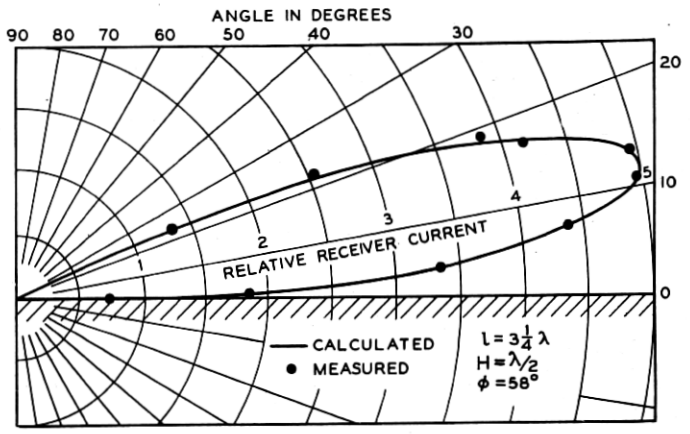

Fig. 14—Receiver current diagram of incident plane directivity with test antenna one-half wave-length above ground. Major lobe only.

discriminate against the components of the received signal. The angle of arrival of these components was measured by the methods described

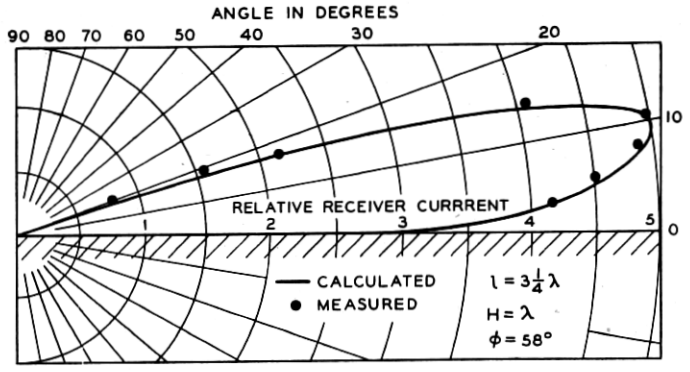

Fig. 15—Receiver current diagram of incident plane directivity with test antenna one wave-length above ground. Major lobe only.

by Friis, Feldman and Sharpless.[2] The agreements were at all times close. This work was incidental to some fading studies the results of which also checked qualitatively the directivity calculations.

These substantial agreements between calculated and measured values are an indication of the accuracy secured in theoretically predicting antenna directivity when using the stated assumptions. It is believed, therefore, that they establish the validity of the design methods now being used for commercial applications of this type of antenna.

Standing Wave Suppression

To obtain the uni-directional characteristics usually desired and to provide a constant terminal impedance over a broad frequency range, the end of the rhombic antenna, remote from the receiver, is terminated in its equivalent characteristic impedance to prevent wave reflections.

The termination was originally adjusted by determining the greatest front-to-back signal reception ratios which could be obtained with the terminating graphite resistors or the other circuits employed. This method of testing proved both cumbersome and erratic for the following reasons:

Radiating field oscillators had to be placed at sizable distances both in front and in the rear of the antenna. Manipulating these oscillators, for frequency runs, proved inconvenient. Furthermore, properly elevating the oscillators was impractical because of the large heights required to simulate the actual average wave-angles usually encountered. When the oscillators were at more reasonable heights above ground, the front-to-back signal ratios could rarely be reproduced since the wave-direction was unstably situated on the lower steep edge of the incident plane directive diagram.

The procedure for testing the termination has been simplified through the measurement, by a substitution method, of the antenna terminal impedance as the frequency is varied over the required frequency band. By readjusting the termination, until these measured values are constant, the required value is obtained.

The schematic diagram of the impedance measuring equipment employed is shown in Fig. 16. In the actual apparatus, the individual

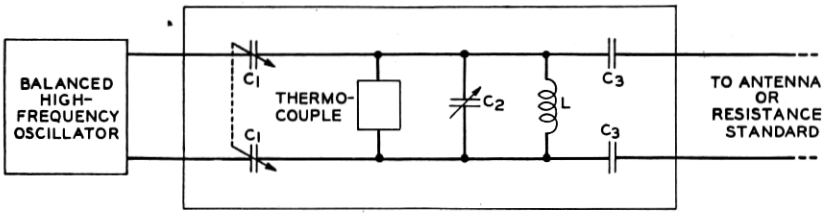

Fig. 16—Schematic diagram of impedance measuring equipment.

parts are separately shielded and symmetrically arranged so that the assembly can be attached to a portable balanced oscillator used for other work. Such a combination is shown in the photograph of Fig. 17.

Again referring to Fig. 16, the condensers marked C_1 control the degree of coupling while maintaining an accurate balance to ground.

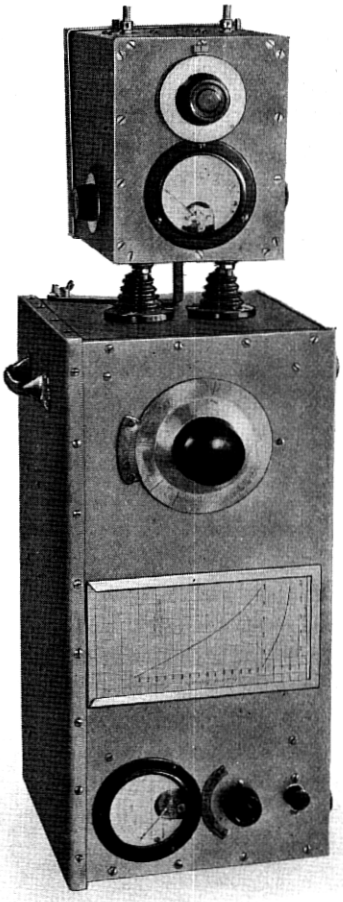

Fig. 17—Impedance measuring equipment and balanced oscillator.

C_2 is a condenser used for anti-resonating the complete circuit, this anti-resonance being indicated by a thermocouple deflection. The condensers labelled C_3 are large blocking condensers which have been added to the circuit to permit the measurement of the value of the variable substitution resistance without the necessity of disconnecting that resistance. A pencil lead is usually employed as this resistor.

The measurement consists in replacing the antenna by a value of resistance R which gives the same thermocouple deflection. The reactive components involved are tuned out in each case by adjusting the condenser C_2. The change in the dial setting of this condenser, as the resistance is substituted for the antenna, permits the determination of the reactive component of the antenna impedance.

Curve 3, in Fig. 18, shows the terminal resistance versus frequency of a properly terminated experimental antenna constructed by the authors. Curve 1, of that figure, results from a termination resistance which is too large while that in curve 2 is too small. Incidentally, it is interesting to note that the value of the measured terminal resistance of this antenna is lower than the resistance required, at the other end of the antenna, for the correct termination. This behavior is probably an effect of the radiation resistance of the system.

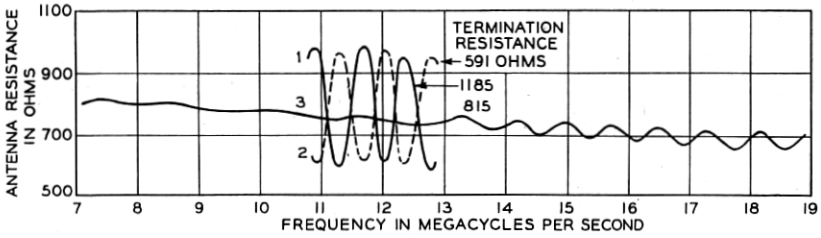

Fig. 18—Rhombic antenna resistance versus frequency for three values of termination resistance.

When a lumped termination resistance is employed, measurements reveal that it operates as if paralleled by a small effective capacitance, a capacitance probably due to the proximity of the adjacent converging antenna wires. This capacitance prevents the resistance from acting as an entirely satisfactory termination. Its effect can be minimized through a proper distribution of the termination resistance over a short length of the converging part of the antenna. This distribution tends to isolate the harmful capacitances by means of the resistances and also introduces a small effective series inductance which is helpful in neutralizing the residual capacitive reactance. Other circuits have been devised, but this one is often employed because of its simplicity and ruggedness.

Antenna-to-Pipe Line Coupling Circuits

Concentric pipe transmission lines are usually favored for receiving antenna installations as they can be buried in the ground to give a substantial and weather-proof construction, free from reactions on adjacent antennas. This pipe-line runs up one pole of a rhombic

antenna and terminates adjacent to the output terminals of the antenna.

Large terminated rhombic antennas, built with number 12 A.W.G. wire, present a terminal impedance, balanced to ground, of nearly 800 ohms resistance. Where the ratio of the inner diameter of the outer pipe to the outer diameter of inner pipe of the transmission line is the optimum value [5] of 3.6, the characteristic impedance of the line is about 77 ohms. The problem is, therefore, to transform properly a balanced resistance of about 800 ohms into an unbalanced resistance of about 80 ohms without appreciable losses over the entire operating range of the antenna.

Figure 19 is a photograph of a simple type of coupling circuit developed for experimental use. Figure 20 is the measured loss versus frequency curve obtained when the device is connected between the stated impedances. The broad frequency range is primarily the result of a high coefficient of coupling. Balance is obtained by symmetrically disposing two primary windings in series about two secondary windings in parallel. A still greater operating range may be obtained through a more elaborate arrangement. Note in Fig. 19 that the boxes and pipe line are gas tight so that nitrogen pressure can be applied, if desired, to prevent moisture absorption through "breathing."

Conclusion

The original paper [1] on rhombic antennas, in discussing the situation regarding short-wave communication, stated that the main limitations in this field were three in number:

(*a*) Inherent receiver noise.
(*b*) External noise (static, man-made noises, etc.)
(*c*) Signal fading.

That paper attempted to show that the design of the receiving antenna system has an important bearing upon overcoming all three of these difficulties.

In the present paper, the authors have indicated how progress in overcoming the first two limitations, through refinements in the horizontal rhombic type of antenna, has been made.

Improvements in the selection of the receiving antenna dimensions have greatly helped the noise situation. Termination and coupling circuit developments now allow many of these antennas to operate one circuit or several circuits simultaneously within a four-to-one frequency range.

[5] E. J. Sterba and C. B. Feldman, "Transmission Lines for Short-Wave Radio Systems," *Proc. I. R. E.*, July, 1932; *Bell Sys. Tech. Jour.*, July, 1932.

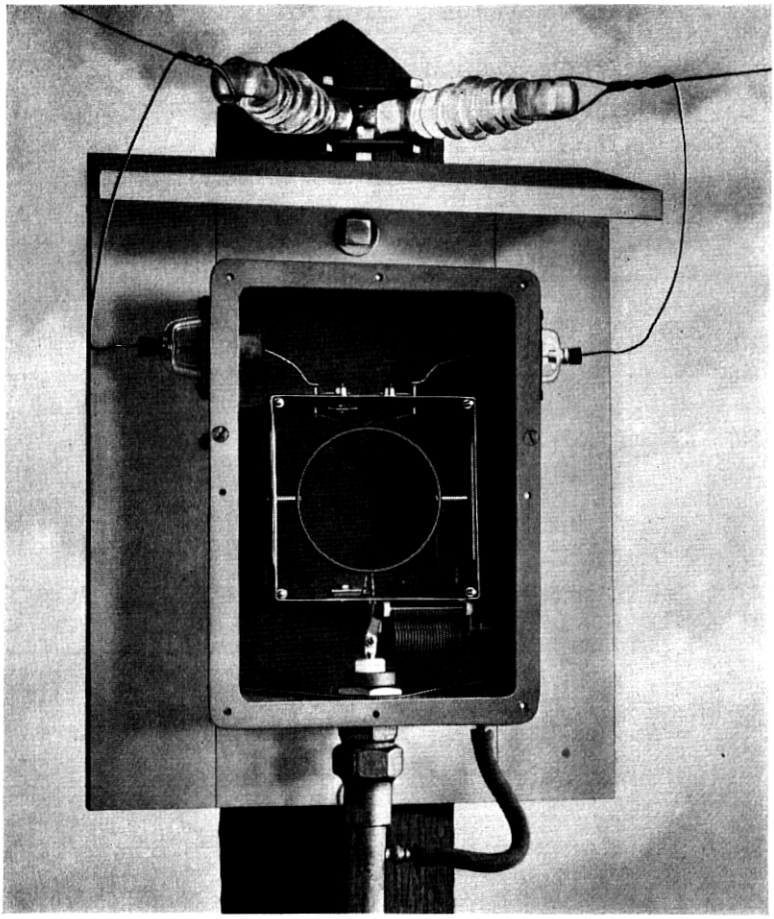

Fig. 19—Experimental equipment for coupling a rhombic antenna to a concentric pipe transmission line.

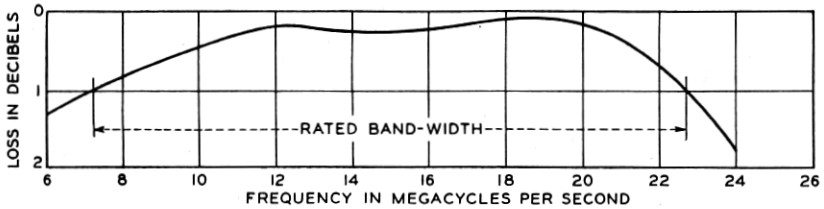

Fig. 20—Loss versus frequency of the experimental coupling equipment, shown in Fig. 19, when used to connect an antenna balanced impedance of 778 ohms in parallel with 5 mmf. to a pipe-line unbalanced resistance of 80 ohms.

APPENDIX

Calculations of Three-Dimensional Directivity

Antenna: Horizontal Rhombus.
Wave Polarization: Horizontal.
Far End Termination: Characteristic Impedance.
Ground Constants: General Case.

Assumptions: Negligible Wire Attenuation and Leakage.
Negligible Mutual Coupling.
Uniform Characteristic Impedance.

Nomenclature: (See Fig. 1)

P = point under consideration.

l = element length.

ϕ = one-half of side apex angle.

Δ = angle made with ground by wave-direction in incident plane.

β = angle made by horizontal component of wave-direction with principal axis drawn through receiver and termination.

H = height above ground.

X = wire distance of point P from R for element (2) as well as for element (1).

ϵ = r.m.s. space voltage.

E = r.m.s. space voltage and phase at P due to ϵ, direct propagation.

E' = r.m.s. space voltage and phase at P due to ϵ, after ground reflection.

E_{P1} and E_{P2} = wire voltage at P in element (1) or element (2), direct propagation.

E_{P1}' and E_{P2}' = same as above but for ground reflection.

a = amplitude ratio of ground reflection to direct space voltage.

α = apparent phase angle change after ground reflection.

λ = wave-length.

I_R = receiver current.

Z_0 = characteristic impedance.

R = receiver impedance.

T = far end termination impedance.

Voltages Induced in Wire:

For a directly propagated wave in element (1), R being the reference point for phases,

$$E_{P1} = \epsilon \cdot \cos(\phi - \beta) \cdot e^{+j\frac{2\pi}{\lambda} \cdot \sin(\phi - \beta) \cdot \cos\Delta \cdot X} dX.$$

For reflected wave in element (1) ($X = 0$ to l)

$$E_{P1}' = a \cdot \epsilon \cdot \cos(\phi - \beta) \cdot e^{+j\left\{\frac{2\pi}{\lambda}[X \cdot \sin(\phi - \beta) \cdot \cos\Delta - 2H \sin\Delta] - \alpha\right\}} dX.$$

Similarly for element (3) ($X = 0$ to l)

$$E_{P3} = \epsilon \cdot \cos(\phi + \beta) \cdot e^{+j\frac{2\pi}{\lambda} \cdot \sin(\phi + \beta) \cdot \cos\Delta \cdot X} dX.$$

$$E_{P3}' = a \cdot \epsilon \cdot \cos(\phi + \beta) \cdot e^{+j\left\{\frac{2\pi}{\lambda}[X \cdot \sin(\phi + \beta) \cdot \cos\Delta - 2H \sin\Delta] - \alpha\right\}} dX.$$

Also for elements (2) and (4) ($X = 0$ to l) where respective side apexes are now reference points for phases,

$$E_{P2} = -E_{P3} \cdot e^{+j\frac{2\pi l}{\lambda} \cdot \sin(\phi - \beta) \cdot \cos\Delta},$$

$$E_{P2}' = -E_{P3}' \cdot e^{+j\frac{2\pi l}{\lambda} \cdot \sin(\phi - \beta) \cdot \cos\Delta},$$

and

$$E_{P4} = -E_{P1} \cdot e^{+j\frac{2\pi l}{\lambda} \cdot \sin(\phi + \beta) \cdot \cos\Delta},$$

$$E_{P4}' = -E_{P1}' \cdot e^{+j\frac{2\pi l}{\lambda} \cdot \sin(\phi + \beta) \cdot \cos\Delta}.$$

Receiver Current where $T = Z_0$ and $R = Z_0$

$$I_R = \int_0^l \frac{E_{P1} + E_{P1}' + E_{P3} + E_{P3}'}{2Z_0} \cdot e^{-j\frac{2\pi}{\lambda}X} + \int_0^l \frac{E_{P2} + E_{P2}' + E_{P4} + E_{P4}'}{2Z_0} \cdot e^{-j\frac{2\pi}{\lambda}X} \cdot e^{-j\frac{2\pi}{\lambda}l},$$

$$I_R = \int_0^l \frac{\epsilon \cdot \cos(\phi - \beta)}{2Z_0} \cdot \left[1 + ae^{-j\left(\frac{4\pi}{\lambda} H \sin\Delta + \alpha\right)}\right] \cdot e^{-j\frac{2\pi}{\lambda}[1 - \sin(\phi - \beta) \cdot \cos\Delta]X} dX + \int_0^l \frac{\epsilon \cdot \cos(\phi + \beta)}{2Z_0} \cdot \left[1 + ae^{-j\left(\frac{4\pi}{\lambda} H \sin\Delta + \alpha\right)}\right] \cdot e^{-j\frac{2\pi}{\lambda}[1 - \sin(\phi + \beta) \cdot \cos\Delta]X} dX - \int_0^l \frac{\epsilon \cdot \cos(\phi - \beta)}{2Z_0} \cdot \left[1 + ae^{-j\left(\frac{4\pi}{\lambda} H \sin\Delta + \alpha\right)}\right] \cdot e^{-j\frac{2\pi l}{\lambda}[1 - \sin(\phi + \beta)\cos\Delta]} \cdot e^{-j\frac{2\pi}{\lambda}[1 - \sin(\phi - \beta)\cos\Delta]X} dX$$

$$- \int_0^l \frac{\epsilon \cdot \cos(\phi + \beta)}{2Z_0} \cdot \left[1 + ae^{-j\left(\frac{4\pi}{\lambda} H \sin\Delta + \alpha\right)}\right] \cdot e^{-j\frac{2\pi l}{\lambda}[1 - \sin(\phi - \beta)\cos\Delta]} \cdot e^{-j\frac{2\pi}{\lambda}[1 - \sin(\phi + \beta)\cos\Delta]X} dX,$$

$$I_R = \frac{\epsilon \cdot \cos(\phi - \beta)}{2Z_0} \cdot \left[1 + ae^{-j\left(\frac{4\pi}{\lambda} H \sin\Delta + \alpha\right)}\right] \cdot \left[1 - e^{-j\frac{2\pi l}{\lambda}[1 - \sin(\phi + \beta)\cdot\cos\Delta]}\right] \cdot \int_0^l e^{-j\frac{2\pi}{\lambda}[1 - \sin(\phi - \beta)\cdot\cos\Delta]X} dX$$
$$+ \frac{\epsilon \cdot \cos(\phi + \beta)}{2Z_0} \cdot \left[1 + ae^{-j\left(\frac{4\pi}{\lambda} H \sin\Delta + \alpha\right)}\right] \cdot \left[1 - e^{-j\frac{2\pi l}{\lambda}[1 - \sin(\phi - \beta)\cdot\cos\Delta]}\right] \cdot \int_0^l e^{-j\frac{2\pi}{\lambda}[1 - \sin(\phi + \beta)\cdot\cos\Delta]X} dX,$$

$$I_R = +j\frac{\epsilon\lambda}{4\pi Z_0} \cdot \frac{\cos(\phi - \beta)}{1 - \sin(\phi - \beta)\cdot\cos\Delta} \cdot \left[1 + ae^{-j\left(\frac{4\pi}{\lambda} H \sin\Delta + \alpha\right)}\right] \cdot \left[1 - e^{-j\frac{2\pi l}{\lambda}[1 - \sin(\phi + \beta)\cdot\cos\Delta]}\right]\left[1 - e^{-j\frac{2\pi l}{\lambda}[1 - \sin(\phi - \beta)\cdot\cos\Delta]}\right]$$
$$+ j\frac{\epsilon\lambda}{4\pi Z_0} \cdot \frac{\cos(\phi + \beta)}{1 - \sin(\phi + \beta)\cdot\cos\Delta} \cdot \left[1 + ae^{-j\left(\frac{4\pi}{\lambda} H \sin\Delta + \alpha\right)}\right] \cdot \left[1 - e^{-j\frac{2\pi l}{\lambda}[1 - \sin(\phi - \beta)\cdot\cos\Delta]}\right]\left[1 - e^{-j\frac{2\pi l}{\lambda}[1 - \sin(\phi + \beta)\cdot\cos\Delta]}\right],$$

$$I_R = j\frac{\epsilon\lambda}{4\pi Z_0} \cdot \left[\frac{\cos(\phi - \beta)}{1 - \sin(\phi - \beta)\cdot\cos\Delta} + \frac{\cos(\phi + \beta)}{1 - \sin(\phi + \beta)\cdot\cos\Delta}\right] \cdot \left[1 + ae^{-j\left(\frac{4\pi}{\lambda} H \sin\Delta + \alpha\right)}\right] \cdot \left[1 - e^{-j\frac{2\pi l}{\lambda}[1 - \sin(\phi + \beta)\cdot\cos\Delta]}\right]$$
$$\cdot \left[1 - e^{-j\frac{2\pi l}{\lambda}[1 - \sin(\phi - \beta)\cdot\cos\Delta]}\right],$$

which is the final equation including phase relations.